

Multiple reflow study of ball grid array (BGA) solder joints on Au/Ni metallization

W. H. Zhong · Y. C. Chan · B. Y. Wu · M. O. Alam · J. F. Guan

Received: 30 August 2005 / Accepted: 27 January 2006 / Published online: 23 February 2007
© Springer Science+Business Media, LLC 2007

Abstract This paper evaluates the shearing behavior of ball grid array (BGA) solder joints on Au/Ni/Cu pads of FR4 substrates after multiple reflow soldering. A new Pb-free solder, Sn–3Ag–0.5Cu–8In (SACI), has been compared with Sn–3Ag–0.5Cu (SAC) and Sn–37Pb (SP) solders, in terms of fracture surfaces, shearing forces and microstructures. Three failure modes, ball cut, a combination of solder shear and solder/pad bond separation, and pad lift, are assessed for the different solders and reflow cycles. It is found that the shearing forces of the SP and SAC solder joints tend to increase slightly with an increase in the number of reflow cycles due to diffusion-induced solid solution strengthening of the bulk solder and augmentation of the shearing area. However, the shearing forces of the SACI solder joints decrease slightly after four cycles of reflow, which is ascribed to the thermal degradation of both the solder/intermetallic compound (IMC) and IMC/Ni interfaces. The SACI solder joints yield the highest strengths, whereas the SP solder joints give the smallest values, irrespective of the number of reflow cycles. Thickening of the interfacial IMC layer and coarsening of the dispersing IMC particles within the bulk solders were also observed.

Nevertheless, the variation of shearing forces and IMC thickness with different numbers of reflow cycles was not so significant since the Ni under layer acted as an effective diffusion barrier. In addition, the initially-formed IMC layer retarded the further extensive dissolution of the pad material and its interaction with the solder.

Introduction

During the past few decades, numerous Pb-free solders have been developed, among which the Sn–Ag–Cu alloy system has emerged as one of the promising Pb-free solders with a melting point around 217°C [1, 2]. Even so, the continuous demands for better materials always drive the industry and academic community to search for more, new Pb-free alloys. Recently Hwang proposed that the Sn–Ag–Cu–In solder offers good solderability with a low melting range more close to the melting point of the eutectic Sn–Pb (183°C). The fatigue resistance of solder joints made with it is also excellent [3]. Moreover, alloying with In is believed to increase the compliance as well as the tolerance against contamination. These attributes are rather attractive because this novel solder may achieve Pb-free substitution without markedly changing the conventional reflow soldering temperature, related materials and supporting equipment. This saves in the total manufacturing costs with a higher soldering quality yield, but less modification of the present facilities and technologies. However, reliability data available on this new solder are limited.

W. H. Zhong · Y. C. Chan (✉) · B. Y. Wu · M. O. Alam
Department of Electronic Engineering, City University of Hong Kong, 83 Tat Chee Avenue, Kowloon, Hong Kong, P.R. China
e-mail: eeycchan@cityu.edu.hk

J. F. Guan
Department of Mineral Processing, Wuhan University of Science and Technology, Wuhan, P.R. China

In order to preserve the solderability of the pads, it is critical to cover bare Cu pads with coatings, which act as a protector against oxidation during storage and a diffusion barrier during soldering. Various materials such as organic chemicals, pure Sn, pure Ag, and different combinations of Ni, Pd and Au have been suggested as coating for Cu pad [4]. However, Sn gives a possible problem with whisker formation, Ag can contribute to difficulties with electromigration and Pd is expensive. Thus metallization with Au/Ni as a replacement of hot air solder leveling (HASL) using Sn–Pb finish has become prevalent [5, 6]. Fortunately, this scheme is ready for Pb-free soldering as a relatively mature technique in current use, with acceptable tradeoff between cost and reliability.

The ball grid array (BGA) package has favored widespread application by virtue of enhancing miniaturization and performance. Along with the progressive development of electronic interconnection towards smaller size and higher integration, the mechanical integrity of solder joints is essentially a serious reliability concern. So far substantial studies of the mechanical strength of BGA solder joints have been made with respect to different solders, pad and substrate designs, shearing/pulling parameters, reflow ambience and aging conditions. However, few studies have concentrated on the effect of multiple reflow cycles [7–16]. Despite the fact that, BGA solder joints may undergo several cycles of reflow during component manufacturing, soldering and rework processes.

Hence, this study aims to investigate the effect of repeated reflow cycles on the reliability of Sn–3Ag–0.5Cu–8In (SACI) BGA solder joints on the Au/Ni metallization, in comparison with the popular Pb-free solder Sn–3Ag–0.5Cu (SAC) and traditional Sn–37Pb (SP) solder.

Experimental

Three types of BGA solder balls, SACI, SAC and SP (hereafter SACI, SAC and SP), were used each with a diameter of about 760 μm . The SACI solder was identified by differential scanning calorimetric (DSC) measurements to have a melting range of 202–208°C. Three sets of BGA solder joints, were prepared by assembly of the solder balls on the substrate which involved fluxing the substrate, placing the balls onto the pads and reflow soldering. The substrate was a FR4 laminate with pad diameter of 650 μm , but a solder mask opening of about 850 μm . The pads were constructed by immersion Au/electroless Ni metallization, with thicknesses of 0.5 μm Au and 5 μm Ni, over

an underlying Cu layer. The soldering was carried out in five-zone forced convection reflow oven (BTU VIP-70N) with the aid of WS60 paste flux (Alpha Metals). According to the temperature profile obtained from the pads without solder balls, the peak temperature value was 251°C and the times above 183, 202 and 217°C, was about 140, 102 and 82 s, respectively. After the first reflow, all the samples were cleaned for 5 min in alcohol in an ultrasonic bath. Subsequently, the samples were dried and divided into different groups to conduct repeated reflow of 2, 4, 9, 16 and 25 cycles.

The shearing strength of the solder joints was measured using a Dage 4000 model bond tester, with shearing a speed of 500 $\mu\text{m/s}$ and shear height of 150 μm (distance from blade tip to surface of the solder mask). For each case, the average of a total 32 measurements was made, wherein the highest and lowest value were not considered. The fracture surfaces on the substrate side were observed with a Philips XL40 FEG type scanning electron microscope (SEM) machine.

Several samples were cross-sectioned and ground down towards to the middle of the solder joints to characterize the thickness and morphologies of the intermetallic compounds (IMC) formed within the solder joints. The polished surfaces were lightly etched in a 3 vol% HCl aqueous solution. Microstructural and compositional information on the solder joints were obtained with the SEM coupled to an energy dispersive X-ray (EDX) system.

Results and discussion

Failure modes and fracture surfaces

Generally, there are three main failure modes, I, II and III, observed after the shearing tests, as schematically shown in Fig. 1.

Mode I was identified to be complete cut through of the bulk solder balls as illustrated in Fig. 1b. This fracture occurred at a location near but lower than the shearing height (150 μm), leaving a thick layer of solder on the pad. This indicates that the solder/pad bond is much stronger than the shearing strength of the bulk solders.

Mode II is seen as a combination of solder shear and solder/pad bond separation, as illustrated in Fig. 1c. At some region on the pad, the fracture occurs through the solder; meanwhile at other places it is located within the IMC layer. In this case, the solder layer remaining on the pad is much thinner than that for mode I. The cracks are found to propagate along either

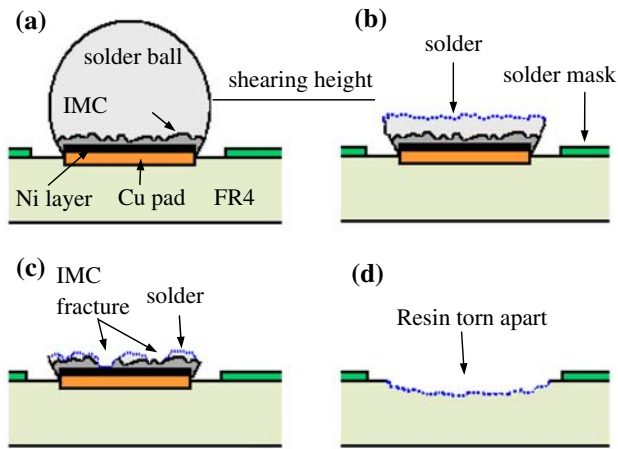


Fig. 1 Schematic drawing of shearing fracture modes of BGA solder joints: (a) shearing setup, (b) mode I, (c) mode II, (d) mode III

the solder/IMC interface or the IMC/Ni interface and within the IMC. It is believed that the shearing strength of the bulk solder is comparable to the adhesive strength of the two interfaces. The brittleness of the thin layer of IMC contributes to the fracture in this location.

Mode III is entirely different in that the whole pad is lifted off, as depicted in Fig. 1d. Due to repeated heating, the textures of the printed circuit board (PCB) base materials degrade dramatically to be weaker than the solder/pad bond and the bulk solder. Therefore, the whole solder joint is maintained intact, whilst the resin under the pad is torn apart to expose glass fibers in the PCB. Although this phenomenon is undesirable, the PCB is likely to experience more thermal damage since higher soldering temperatures and frequent rework are needed for Pb-free processing.

It was confirmed that for up to 16 reflow cycles, the dominant shearing behavior for both the SP and SAC solder joints were mode I. The fracture surfaces of the two solder joints were more or less similar, showing a large ductile deformation of solder, as can be seen from typical topographies in Figs. 2, 3, 4 and 5. Comparing the 1 cycle of reflow with 16 cycles of reflow (Fig. 2 with Fig. 3 and Fig. 4 with Fig. 5), it is obvious that repeated reflow cycles do not affect the morphology substantially. Nevertheless, the results after 16 cycles of reflow exhibit a relatively smaller deformation and somewhat irregular appearance. This is partially because of the increase of Ni diffusion into the solder and coarsening of precipitated IMC particles with increased reflow cycles.

Up to 16 cycles of reflow, the shearing of SACI solder joints primarily follows mode II. Figures 6 and 7 show representative fracture pictures of the SACI solder

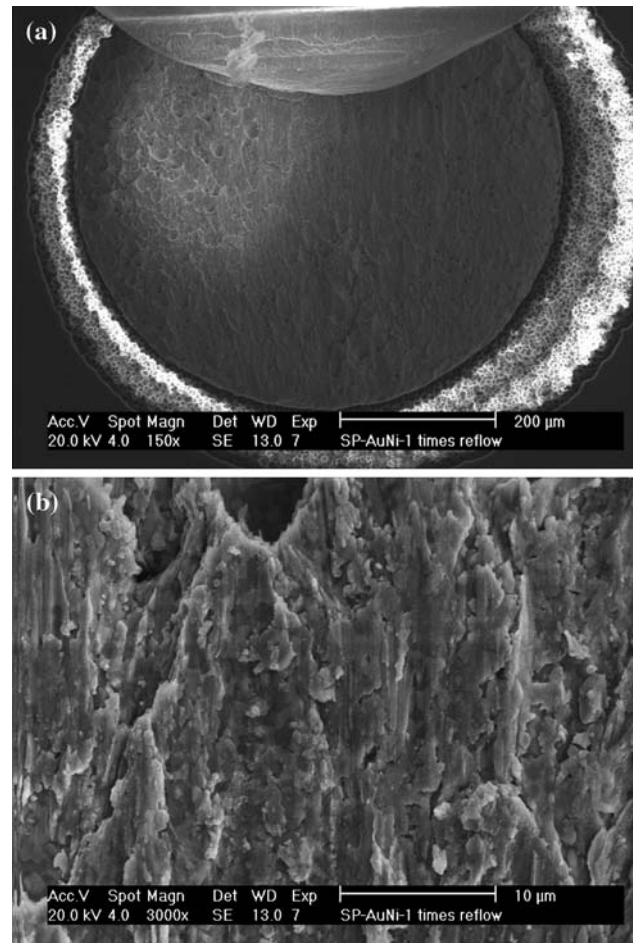


Fig. 2 Typical shearing surfaces of SP solder joints after one cycle of reflow: (a) whole configuration, (b) higher magnification of fracture morphology

joints after 1 and 16 cycles of reflow, respectively. For the one cycle of reflow case, most of the solder at the pad edges are broken away together with the IMC, meanwhile a thin layer of solder remains in the centre part of the pad, as shown in Fig. 6a. A few broken Ni–Cu–Sn IMC particles sporadically scattered on the Ni surface are seen at higher magnification in Fig. 6b. It can be speculated that the crack initiates and propagates at the IMC/Ni interface in an early stage of the shearing; then the fracture path moves to be in the bulk solder when the total area subjected to the load becomes too small to sustain the external load. This case reveals that the shearing strength of the bulk SACI solder is slightly larger than the adhesive strength of the IMC/Ni interface. It also indicates that the solder/IMC interface is more robust than the IMC/Ni interface. This is mainly because the upper surface of the IMC layer is metallurgically more affinitive to the solder than the bottom surface of the IMC to the underneath Ni. Moreover, the solder is mechanically geared by the irregularly shaped

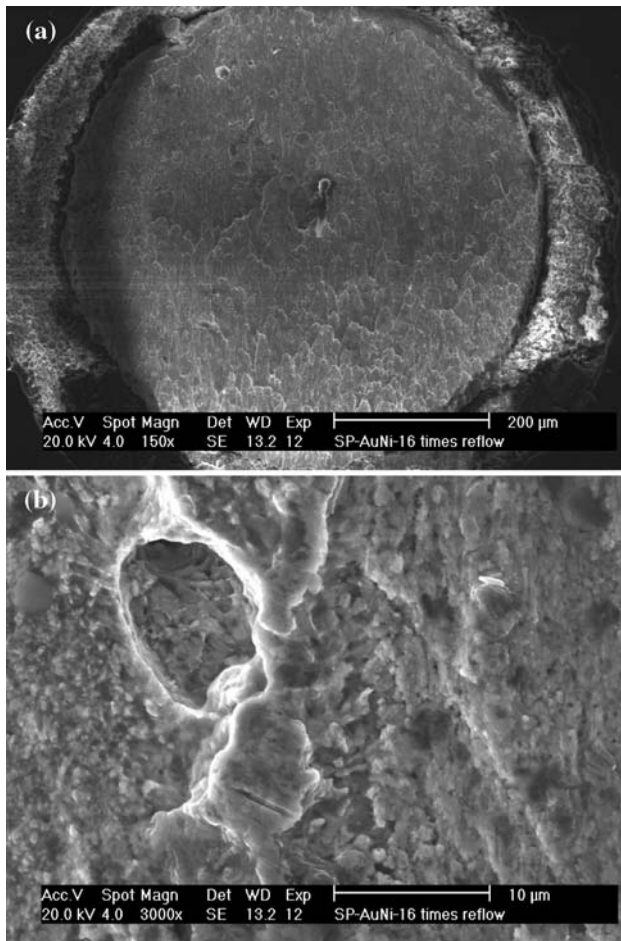


Fig. 3 Typical shearing surfaces of SP solder joints after 16 cycles of reflow: **(a)** whole configuration, **(b)** higher magnification of fracture morphology

IMC layer, whereas the IMC/Ni interface is readily smooth for slip and movement. Furthermore, during the thermal and mechanical history, the solder can absorb more stresses at the solder/IMC interface than can the Ni at the IMC/Ni interface. Finally, the fracture of the brittle IMC and the crack inside the Ni layer may also contribute to the degradation of the IMC/Ni interface adhesion. After 16 cycles of reflow, the shearing test results show less solder residue adhering to the pads, as displayed in Fig. 7a. It is interesting to note from Fig. 7b that a very thin layer of solder remains on top of the IMC layers, where also the cracks in the IMC and Ni layers are observed. The IMC layer is weakened by this type of corrosion crack along the nodule boundaries which are related to the black pad effect of the electroless Ni (P) layer [17]. In addition, many small Ag-rich IMC particles are dispersed on the Ni layer surface. It is thought that excess reflow cycles may not only degrade the adhesion of both the solder/IMC and IMC/Ni interfaces, but also

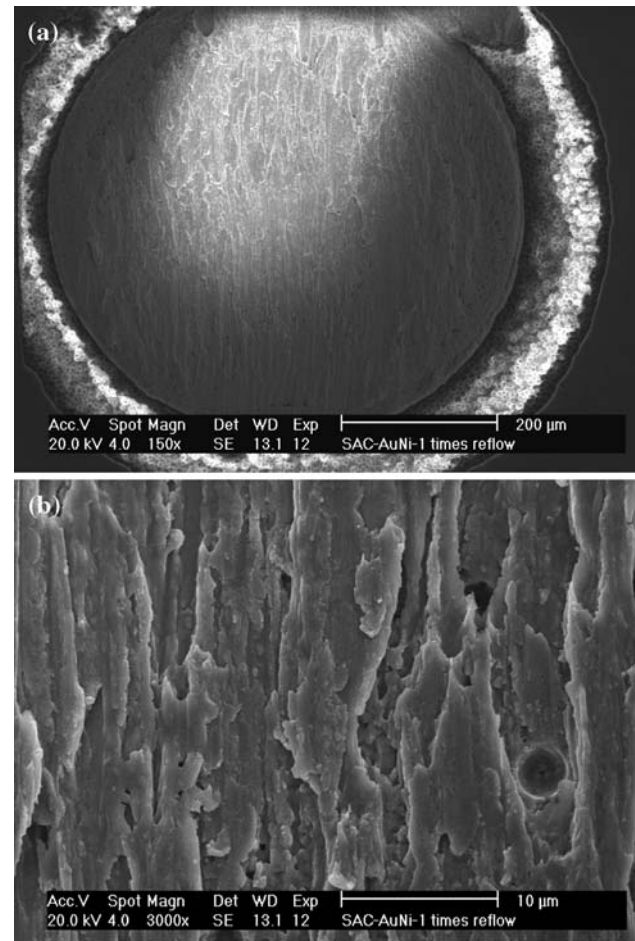


Fig. 4 Typical shearing surfaces of SAC solder joints after one cycle of reflow: **(a)** whole configuration, **(b)** higher magnification of fracture morphology

make the IMC layer flatter. As a result, more of the fracture surface becomes located at the solder/IMC interface, with a smaller area at the IMC/Ni interface.

When the number of reflow cycles is more than 16, more and more shearing failures are found to be mode III, regardless of solder type. Figure 8a shows the shearing result of a 25-cycles-reflowed solder joint where the resin and glass fibers are exposed because the whole Cu pad has been peeled away. This implied that the Cu/resin bond has become weak because the Cu pad absorbs and conducts heat quickly during the repeated reflows. In addition, the large opening of the solder mask contributes to the porous structure, shown in Fig. 8b, making it more vulnerable to the overheating. From this point-of-view, it is expected that solder joints will be more reliable if the solder contact area is more closely defined by the solder mask, i.e. a small portion of the Cu pad is covered by the mask.

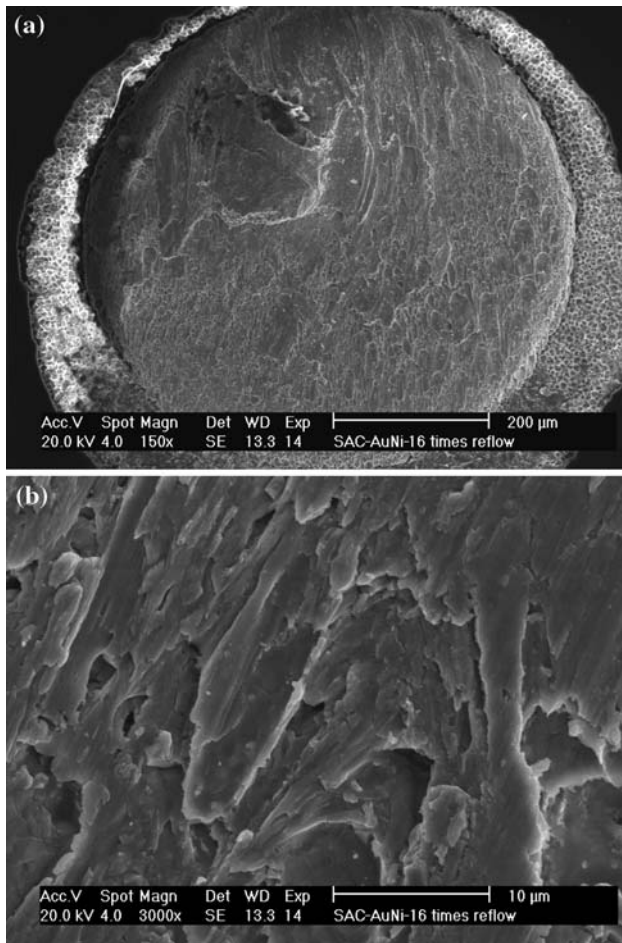


Fig. 5 Typical shearing surfaces of SAC solder joints after 16 cycles of reflow: (a) whole configuration, (b) higher magnification of fracture morphology

Shearing forces

The average shearing forces of the SACI, SAC and SP solder joints are plotted in Fig. 9 with respect to the number of reflow cycles. The shearing forces after 25 cycles of reflow decreased sharply to less than 1,200 g. These unstable values represent the peel strength between the pad and the resin, which are not shown in this figure.

Without doubt, the SACI solder joints yield the highest strengths, whereas the SP solder joints generate the lowest values, irrespective of the number of reflow cycles. The SAC solder joints lie in-between them. It is fortunate that due to a higher Sn content and less ductility, some of the mechanical properties of Pb-free solders are enhanced compared to those of the SP solders [18]. In a separate experiment as shown in Fig. 10, the mean microhardness of the three solder joints is also quite different. There is often a simple

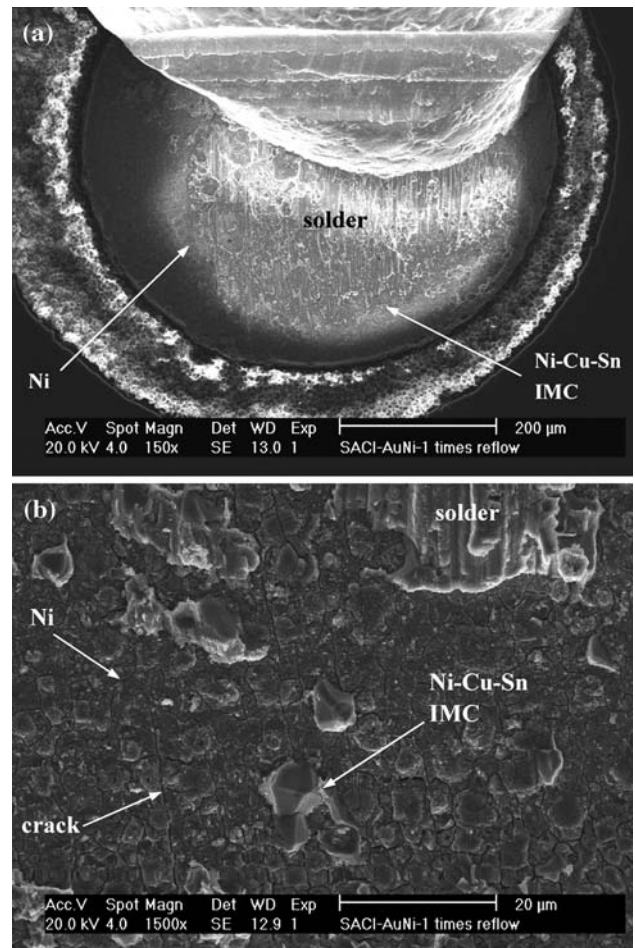


Fig. 6 Typical shearing surfaces of SACI solder joints after one cycle of reflow: (a) whole configuration, (b) higher magnification of fracture morphology

relationship between hardness and strength. Thus SACI would appear to offer enhanced strength due to the assumed substitutional nature of In in Sn. The In solute atoms would be attracted to and interact with both edge and screw dislocations and impede dislocation movement, which increases the strength of the solder [3]. It is also believed that the addition of ‘In’ element to the SAC solder, not only lowers the melting range, but also improves the wettability since ‘In’ is a low melting point, active element. Thus, In can enhance the metallurgical bonding between solder balls and pads. Therefore, significant differences in shearing strength are recorded among the three types of solder joints, especially for the SACI solder.

Although the variation of shearing force with cycles of reflow is not significant for all the solder joints, generally the values for the SP and SAC solder joints increase slightly with an increased number of reflow cycles. It is suggested that repeated reflow cycles

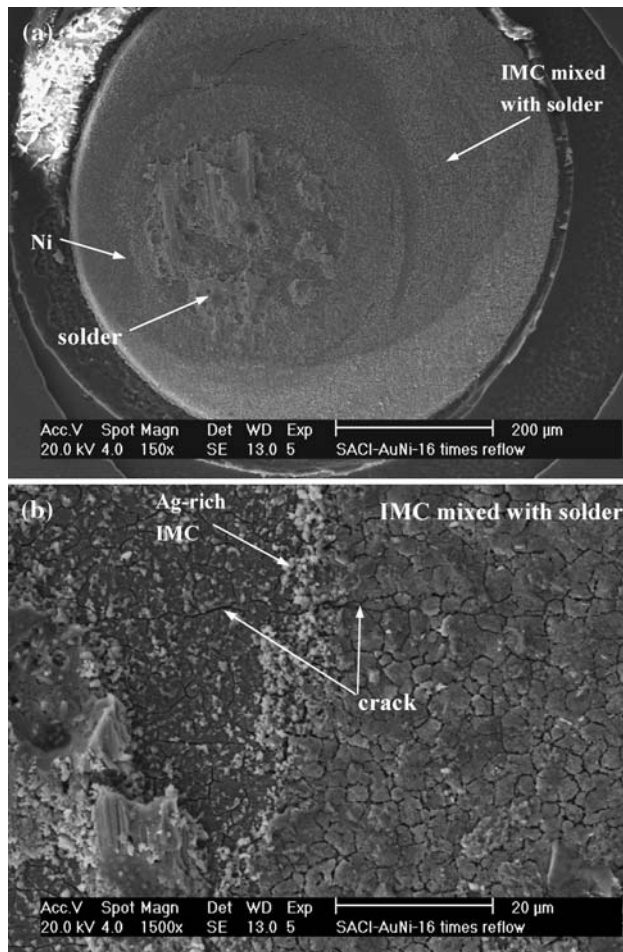


Fig. 7 Typical shearing surfaces of SACI solder joints after 16 cycles of reflow: (a) whole configuration, (b) higher magnification of fracture morphology

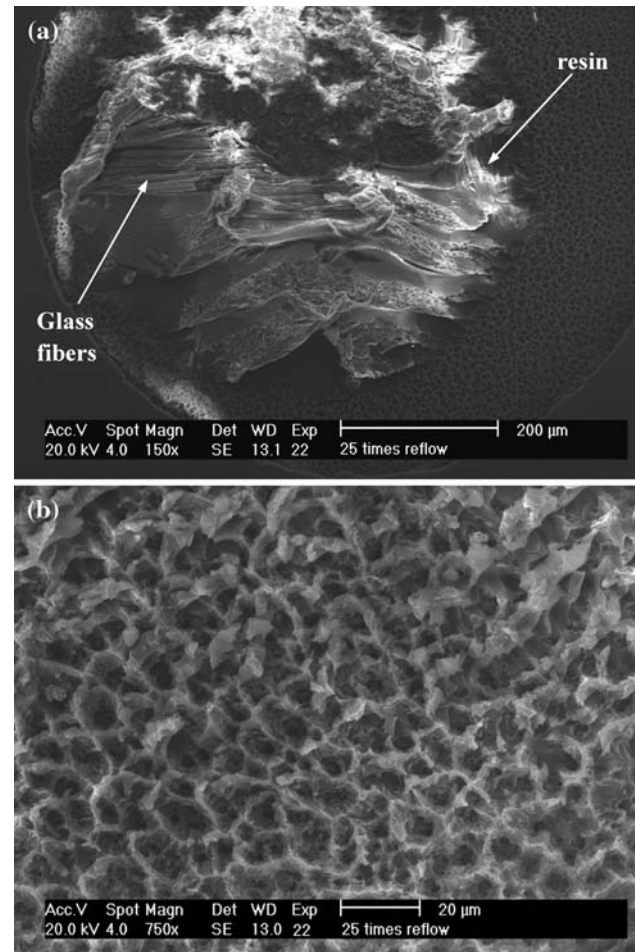


Fig. 8 Representative shearing surfaces of all solder joints after 25 cycles of reflow: (a) whole configuration, (b) higher magnification view of porous resin structure underneath the pad

enlarge the contact area and lower the height of the solder joints. As a result, the forces become higher because of the larger shearing area. Moreover, the multiple reflow process may enhance interdiffusion and interaction between the solders and pad metals, which can induce microstructural changes within the solder joints. It is suggested that during soldering, the thin layer Au dissolves entirely into, and reacts rapidly with, the solders to form homogeneously distributed small brittle AuSn_4 IMC particles [19]. At the same time, some Ni atoms diffuse into the solder. Both processes facilitate an increment of the mechanical strength of the bulk solder. According to the fracture mode analysis described above, the SP and SAC solder joints mainly shear through the bulk solder, while the SACI solder joints fail at both the IMC related interfaces and within the bulk solder. This implies that the degradation of bonds between the IMC and solder and Ni layer may counteract the increase of shearing

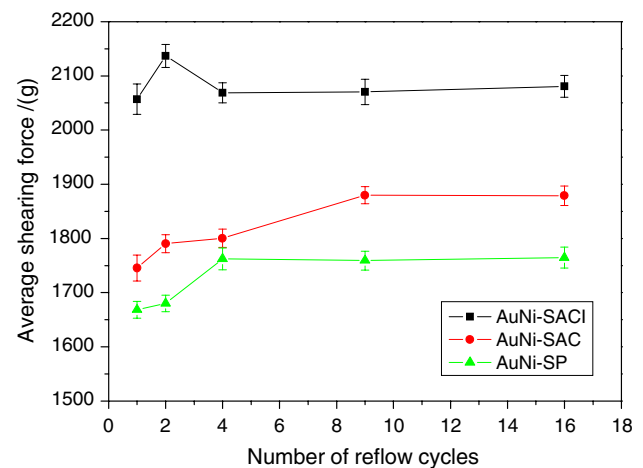


Fig. 9 Variation of average shearing forces of solder joints with respect to different numbers of reflow cycles

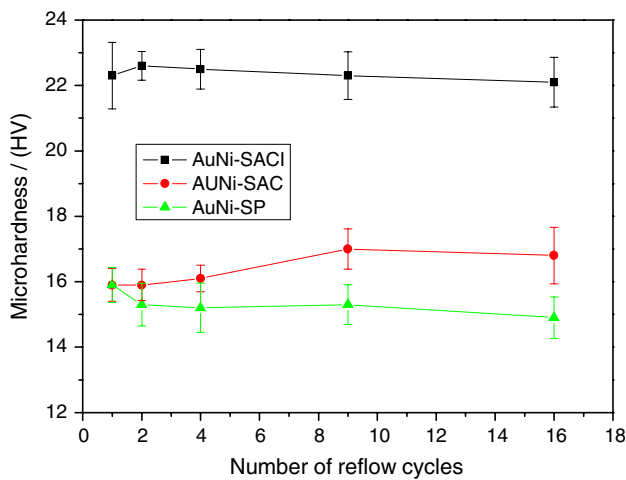


Fig. 10 Microhardness of three types of solder joints with respect to different numbers of reflow cycles

forces contributed by the larger contact area and solute strengthening. This may be why a slight decrease of shearing forces was recorded with SACI solder joints after four cycles of reflow.

All of these effecting influence, if not dramatically, the mechanical behavior of the solder joints. In addition, once the initial IMC layers are formed in the first soldering process, they can retard the extensive dissolution of the pad metals into the solder joints during subsequent reflow treatments.

Cross-section microstructures

Cross-sectional microstructures of the three types of solder joints are shown in Figs. 11, 12 and 13, in which 1 cycle and 16 cycles of reflow are selected for comparison.

Fig. 11 (a) Interfacial microstructure of a SP solder joint after one cycle of reflow. (b) Interfacial microstructure of a SP solder joint after 16 cycles of reflow

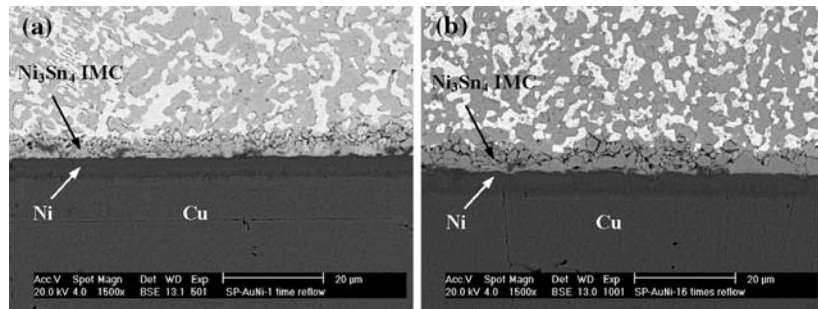


Fig. 12 (a) Interfacial microstructure of a SAC solder joints after one cycle of reflow. (b) Interfacial microstructure of a SAC solder joint after 16 cycles reflow

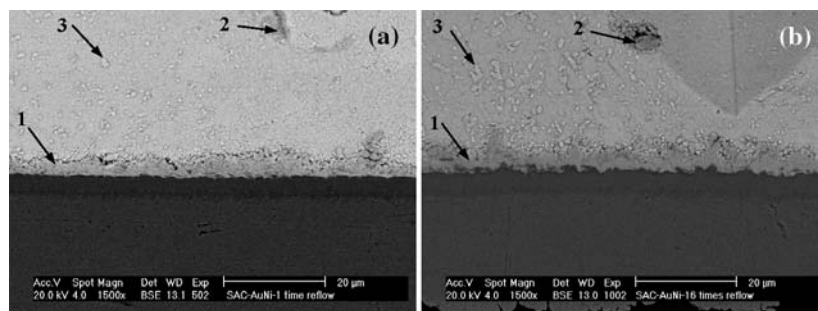
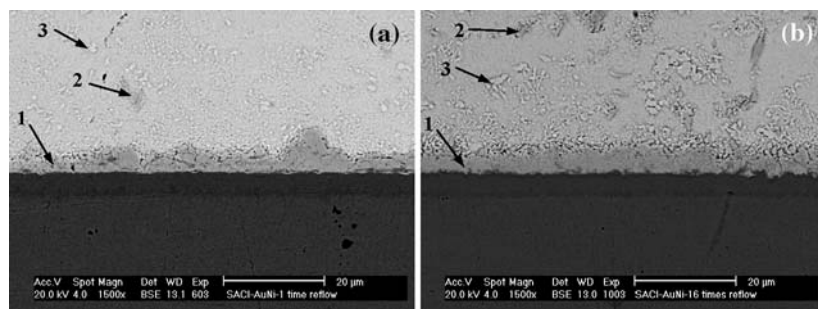


Fig. 13 (a) Interfacial microstructure of a SACI solder joints after one cycle of reflow. (b) Interfacial microstructure of a SACI solder joints after 16 cycles of reflow



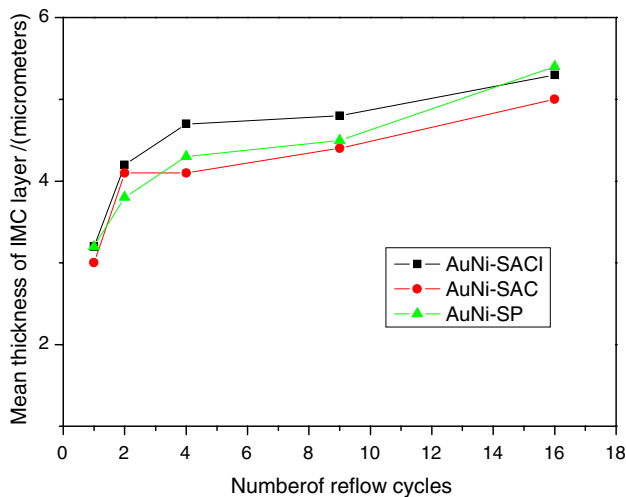


Fig. 14 Mean thickness of IMC layer developed with different number of reflow cycles

In general, the IMC layer formed at the interface after 16 cycles reflow is much denser and thicker than that after 1 cycle of reflow. After repeated melting and solidification of the solder joint, the IMC layer becomes more compact and flatter with a larger grain size. The mean thicknesses of the IMC layer after multiple cycles of reflow are plotted in Fig. 14. The thicknesses of IMC developed by the three types of solder joints are more or less similar and they do not increase substantially after two cycles of reflow, which implies that the initially-formed IMC layers retard further extensive dissolution of the base materials and interaction with the solder. However, the coarsening of the IMC particles embedded within the bulk solder is apparent. The EDX results of the atom percentages of all IMC phases (denoted by 1, 2 and 3) in Figs. 11, 12 and 13 show that with increased number of reflow cycles, the layered IMC at the solder/pad interface tends to dissolve and entrap more base metal atoms (Ni). At the same time, the Cu content of the Cu–Ni–Sn IMC particles dispersed in the bulk solder increases slightly. The Ag atoms in the solder tend to precipitate and thus the content of Ag in the Ag-rich IMC particles solder increase quite a lot after 16 cycles of reflow.

Conclusions

The effect of multiple reflow cycles on the shearing behavior of three types of BGA solder joints on Au/Ni metallization was investigated.

Three failure modes were identified for the different solders and number of reflow cycles. Up to 16 cycles of

reflow, the main fracture mode for both the SP and SAC solder joints was cut through of the bulk solder ball, whereas a mixed mode of solder shear and solder/pad bond separation was found for the SACI solder joints. With 25 cycles of reflow, all the solder joints failed at the interface of the pad/resin, in which the whole pad was entirely pulled away due to degradation of the pad/resin bond caused by overheating.

Although the multiple reflow cycles seem to have less influence on the shearing strength, it is believed that the shearing forces of the SP and SAC solder joints tend to increase because of solute strengthening by interdiffusion and shearing area augmentation. Also, for the case of SACI solder joints, the repeated heating causes thermal stress accumulation at both the solder/IMC and IMC/Ni interfaces, which makes the shearing strength decrease slightly. Nevertheless, the SACI solder joints yield the highest strengths, whereas the SP solder joints exhibit the lowest values, irrespective of the number of reflow cycles.

After the microstructural analysis, it was confirmed that the initially-formed IMC layer retards the further extensive dissolution of the pad material and its interaction with the solder. As a result, the thickness of the IMC layer does not increase much even after 16 cycles of reflow. Coarsening and precipitation of IMC particles dispersed within the bulk solders were also detected. However, these had little effect on the shearing strength of the solder joints since the diffusion of Ni into the solder joints is limited.

Acknowledgements This project has been supported by CityU CERG project (9040887, CityU 1106/04E). The authors wish to thank Prof. & Mrs. Brian Ralph at Brunel University for their hard work and great help.

References

- Richards BP, Levoguer CL, Hunt CP, Nimmo K, Peters S, Cusack P (1999) An analysis of the current status of lead-free soldering, (NPL, ITRI and DTI joint report about Pb-free soldering, Jan.). <http://www.npl.co.uk/ei/documents/pbfree-report.pdf>
- Suganuma K (2003) Lead-free soldering in electronics: science, technology and environmental impact. Marcel Dekker, New York
- Hwang JS (2001) Environment-friendly electronics. lead-free technology. Electrochemical Publications, New York, pp 277
- Sattiraju SV, Dang B, Johnson RW, Li YL, Smith JS, Bozack MJ (2002) IEEE Trans Compon Packag Manuf Technol Part C Manuf 25:168
- Connell JO (2005) Study and recommendations into using lead free printed circuit board finishes at manufacturing in circuit test stage (Agilent Technologies white paper). http://www.home.agilent.com/upload/cmc_upload/All/5989-1558EN.pdf

6. Toleno B (2003) PCB surface finish options for lead-free manufacturing, EMS 5. <http://www.emsnow.com/npps/story.-cfm?ID=9784>
7. Li M, Zhang F, Chen WT, Zeng K, Tu KN, Balkan H, Elenius P (2002) *J Mater Res* 17:1612
8. Alam MO, Chan YC, Tu KN (2004) *J Mater Res* 19:1303
9. Huang XJ, Lee SWR, Yan CC (2002) In: Electronic components and technology conference, proceedings of the 52nd ECTC on 28–31 May, California, USA, pp 968
10. Chong V, Lee TK, Lim CT, Gunawan DK (2004) In: Electronics packaging technology conference, proceedings of 6th EPTC on 8–10 December, Singapore, pp 735
11. Yoon W, Kim SW, Jung SB (2005) *J Alloys Compd* 391:82
12. Aderspm IE, Harringa JL (2004) *J Electr Mater* 33:1485
13. Erich R, Richard JC, Wenger GM, Primavera A (1999) In: Proceedings of the 24th IEEE/CPMT international electronics manufacturing symposium on 18–19 October, Austin, TX, USA, pp 16
14. Lim ACP, Kheng LT, Alamsjah A (2003) In: Happy, electronics packaging technology conference, proceedings of 5th on 10–12 December, Pan Pacific Hotel, Singapore, pp 563
15. Fan JW, Kou CT, Yip MC (2003) In: Electronics packaging technology conference, proceedings of 5th on 10–12 December, Pan Pacific Hotel, Singapore, pp 712
16. Anand A, Mui YC, Weidier J, Diaz N (2004) Electronics packaging technology conference, proceedings of 6th on 8–10 December, Pan Pacific Hotel, Singapore, pp 335
17. Roger J, Kwong A (2001) Dealing with the “Black Pad Defect”—a failure analyst perspective, Solectron Corporation Milipitas, CA 95035. <http://www.smta.org/files/jrml0702-roepsch.pdf>
18. Siewert T, Liu S, Smith DR, Madeni JC (2002) Database for solder properties with emphasis on new lead-free solders (report on properties of lead-free solders, release 4.0, National Institute of Standards and Technology & Colorado School of Mines)
19. Kim PG, Tu KN (1998) *Mater Chem Phys* 53:165